systems

MDPI

Article

Carbon, Climate, and Collapse: Coupling Climate Feedbacks and Resource Dynamics to Predict Societal Collapse

Greta Savitsky [1,*], Grace Burnett [2] and Brian Beckage [1,3]

[1] Department of Plant Biology, University of Vermont, Burlington, VT 05405, USA
[2] Department of Environmental Sciences, University of Vermont, Burlington, VT 05405, USA
[3] Department of Computer Science, University of Vermont, Burlington, VT 05405, USA
* Correspondence: gsavitsk@uvm.edu

Abstract

Anthropogenic climate change threatens production of essential natural resources, including food, fiber, and fresh water, and provisioning of ecosystem services such as carbon sequestration, increasing the risk of societal collapse. The Human and Nature Dynamics (HANDY) model simulates the effect of resource overexploitation on societal collapse but lacks representation of feedbacks between climate change and resource regeneration in ecological systems. We extend the HANDY model by integrating models of climate change and ecological function to examine the risk of societal collapse. We conducted a sensitivity analysis of our expanded model by systematically varying key parameters to examine the range of plausible socio-ecological conditions and evaluate model uncertainty. We find that lowered greenhouse gas emissions and resilient ecosystems can delay societal collapse by up to approximately 500 years, but that any scenario with greater than net-zero greenhouse gas emissions ultimately leads to societal collapse driven by climate-induced loss of ecosystem function. Reductions in greenhouse gas emissions are the most effective intervention to delay or prevent societal collapse, followed by the conservation and management of resilient ecological systems to sequester atmospheric carbon.

Keywords: climate; global change; feedbacks; human-nature dynamics; societal collapse; carrying capacity

check for updates

Academic Editor: Oz Sahin

Received: 1 July 2025
Revised: 12 August 2025
Accepted: 19 August 2025
Published: 22 August 2025

Citation: Savitsky, G.; Burnett, G.; Beckage, B. Carbon, Climate, and Collapse: Coupling Climate Feedbacks and Resource Dynamics to Predict Societal Collapse. *Systems* **2025**, *13*, 727. https://doi.org/10.3390/systems13090727

Copyright: © 2025 by the authors. Licensee MDPI, Basel, Switzerland. This article is an open access article distributed under the terms and conditions of the Creative Commons Attribution (CC BY) license (https://creativecommons.org/licenses/by/4.0/).

1. Introduction

Resource consumption and greenhouse gas (GHG) emissions have accelerated since the onset of industrialization, driving the potential for societal collapse. Overshooting the carrying capacity of the natural environment, or overutilization of natural resources to the point of scarcity, has been a common cause of societal collapse in the past. Surpassing carrying capacity has been studied by many academics [1–5], notably coined as Malthusian catastrophe [6], Tragedy of the commons [7], and overshoot and collapse [8]. Some modern scholars believe that modern society may have already reached that point [9,10].

Motesharrei et al. present a conceptual and mathematical model to simulate and study the factors associated with such collapse [1]. Their Human and Nature Dynamics (HANDY) model examines how class inequality and income distribution may affect trends of population dynamics and societal collapse. The HANDY model recreates two patterns of societal collapse driven by inequality and resource overuse and shows that collapse can be avoided when resource depletion and social inequality are low [1]. While HANDY

explores the effect of societal inequity on societal collapse, it does not consider the feedback between anthropogenic climate change and ecosystem function.

Contemporary society faces even greater challenges from environmental change than past collapsed societies [11]. Anthropogenic climate change can induce a reinforcing feedback that alters the potential for ecological systems to sequester carbon. These feedbacks can reinforce climate change through altered disturbance regimes, decreased ecosystem function, and decreases in carbon sequestration capacity [12–15]. Changing temperature associated with climate change has already led to phenological mismatches, range shifts, biodiversity loss, extinctions, and loss of crop photosynthetic capacity [13,16], all of which reduce carbon sequestration and access to ecosystem services. Declines in ecosystem services could drive societal derailment, i.e., disruption of social and economic systems and declines in human population, leading to reductions in anthropogenic GHG emissions through reductions in economic activity, in a balancing feedback that could reduce the rate of climate change [17].

HANDY does not represent this potential feedback between climate change and ecosystem function that could contribute to societal collapse. We represent this missing component by expanding the HANDY model to include a simple climate model [18] and a feedback between climate and ecosystem function in the carbon, climate, and collapse (or C^3) model. We use carbon emissions as a proxy for GHG emissions and carbon intensity (I_C)—Defined as carbon use per unit of wealth accumulation—As a proxy for a society's balance of fossil fuel and renewable energy sources. Our model represents the declining capacity of ecosystems to sequester carbon with climate change, along with reduced regeneration of ecosystem services, reflecting potential declines in production of food, fiber, fresh water, and other vital ecosystem services. We use the yearly change in global mean surface temperature as a proxy for climate change and refer to the two interchangeably throughout this paper.

We use the expanded model of human and ecological dynamics to evaluate how carbon intensity and ecological resilience influence societal dynamics and the risk of societal collapse. Our simulations vary four key parameters to capture uncertainty in carbon intensity and ecological resilience: (1) *Carbon intensity* (I_C), or the degree of societal reliance on fossil fuels versus renewable energy sources, (2) *ecological niche breadth* (σ), which determines ecosystem resilience to changes in climate, (3) *maximum carbon sequestration* (S_{rM}), representing the greatest rate of atmospheric carbon that ecosystems can remove under optimal temperature conditions, and (4) the *functional relationship* (r) between ecosystem resilience and climate change to reflect how ecosystem function may decline as temperature rises. We assess societal resilience to feedbacks between climate change and ecosystem function using collapse or time to collapse in simulations while factorially varying model parameters to assess model sensitivity to parameter uncertainty.

2. Materials and Methods

The HANDY model was created to simulate societal collapse [1]. It uses the predator-prey model [19,20] to investigate human and nature dynamics (Equations (A1)–(A4)) such that the human population serves as "predator" while nature serves as "prey", and humans "predate" on natural resources to grow their population (see Appendix A.1). HANDY expands on this concept by introducing complexity through class stratification and wealth accumulation. It includes two populations of humans: commoners, who use natural resources to generate wealth, and elites, who consume this wealth to increase their population (see Appendix A.2). Motesharrei et al. use the HANDY model to explore how social structures and scales of resource depletion influence societal dynamics (Equations (A5)–(A13)) [1].

Their simulations run for 1000 years and show that societies of all levels of inequality can collapse or reach equilibrium, depending on resource usage.

The climate component of C^3 is designed to capture the change in global mean surface temperature as a function of changing atmospheric carbon (Figure 1). This model element consists of a gray atmosphere radiative transfer module and a temperature simulation module [18]. The atmosphere component computes the net solar flux at the Earth's surface as a function of planetary albedo, incoming solar radiation, and atmospheric opacity (Equations (A14)–(A19)). Then, the temperature module uses this net solar flux to calculate the global mean surface temperature and the difference from the previous year (see Appendix A.3).

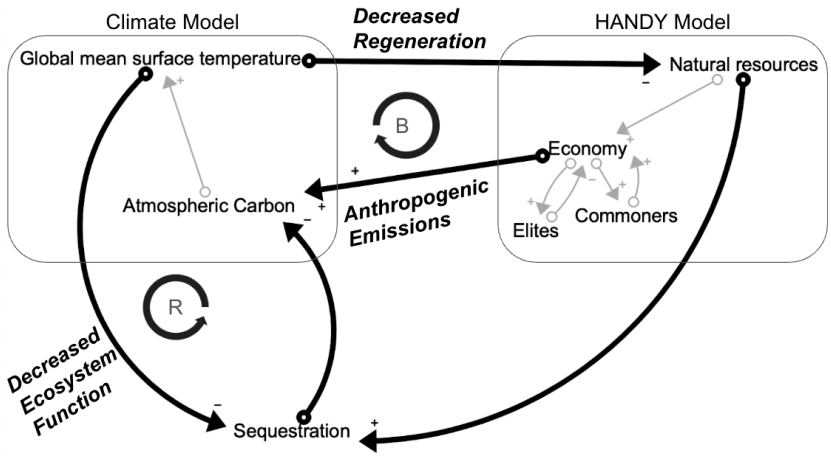

Figure 1. Causal loop diagram illustrating the original HANDY model [1] (right, gray lines), the original climate model [18] (left, gray lines), and C^3 additions (black lines and labels). Two competing feedbacks are denoted by circular arrows: (1) A reinforcing feedback (R) between climate, atmospheric carbon, and sequestration capacity, where climate change reduces the capacity for carbon sequestration, leading to additional climate change and (2) A balancing feedback (B) among climate, natural resources, and the human system, where climate change reduces ecosystem function, reducing the capacity for economic growth, which reduces carbon emissions and resultant climate change.

In our C^3 model, we use the HANDY equitable society scenario, initializing our joint HANDY-climate model with a ratio of 4:1 commoners to elites, starting populations of 100 commoners and 25 elites, and an inequality factor of 1 (with no difference in commoner and elite salaries). Because the society is equitable, with equal pay for commoners and elites, our model does not include wealth inequality, only labor inequality. Following Motesharrei and colleagues, our simulations were 1000 years long to explore both the long-term and near-term consequences of GHG emissions from fossil fuel usage. We added temporal specificity by beginning in the year 1850 to simulate the rise in industrialization and GHG emissions.

The HANDY and climate models are joined through the creation of an atmospheric carbon stock (Figure 1). Atmospheric carbon (A_C) is initialized at 501 PgC, the equilibrium value for the climate model. A_C is increased through carbon emissions and decreased through sequestration:

$$DA_C/dt = E - S \quad (1)$$

Emissions are proportional to the amount of accumulated wealth and the carbon intensity (I_C) of the society, or the amount of carbon in petagrams emitted per ecodollar of accumulated wealth (w):

$$E = I_C \times w \quad (2)$$

Carbon intensity thus represents the "greenness" of a society. Lower values of carbon intensity correspond to a society that relies less on fossil fuel consumption. Higher values correspond to heavy reliance on fossil fuels to generate wealth.

We define ecosystem resilience to include three distinct parameters: σ, r, and S_{rM}. Each parameter represents a facet of resilience and robustness of ecosystem function to climatic change, represented as temperature change. The critical thermal maximum, or σ, refers to the temperature at which ecosystem function ceases, defining the range of temperature niche breadth. This parameter controls the regenerative capacity of natural resources by modifying ecological carrying capacity. Therefore, σ encompasses both niche breadth and regenerative capacity. In addition, we explore the conservation of ecosystem function through varying two carbon sequestration parameters (r and S_{rM}). S_{rM} is the maximum sequestration rate, representing the maximum amount of carbon that can be removed from the atmosphere per year per unit of ecosystem resources when the ecosystem is at its optimal climate condition (e.g., optimal temperature).

Sequestration, or the removal of carbon from the atmosphere through photosynthesis, is proportional to the amount of available natural resources (y) as a proxy for ecosystem services and the sequestration rate, (S_r), or the amount of carbon sequestered per year by one ecodollar of natural resources (Figure 1). This assumes that natural resources represent Earth's photosynthesizing vegetation:

$$S = S_r \times y \tag{3}$$

Sequestration rate changes with change in temperature (ΔT), as increasing temperature can put stress on vegetation through reduction in photosynthetic capacity, as well as phenological mismatch, range shift, biodiversity loss, or even extinction [13,21]:

$$S_r = S_{rM} \times (1 - \Delta T/6)^r \tag{4}$$

where r is a steepness parameter used to control the functional relationship between temperature and sequestration, and S_{rM} is the maximum amount of carbon that can be sequestered at the optimal temperature, or ΔT = 0. The steepness parameter (r) represents the possible functional forms of how temperature can reduce the photosynthetic capacity of vegetation, such that $(1 - \Delta T/6)^r$ equals a number between 0 and 1 to modify the photosynthetic rate as ΔT increases from 0. Steepness can be varied to explore these functional relationships. This introduces a reinforcing feedback whereby increasing atmospheric carbon creates higher temperatures, making the sequestration capacity of ecosystems lower, leading to even more atmospheric carbon (Figure 1).

Temperature change (ΔT) can also affect the ability of ecosystems to regenerate after being utilized for the production of wealth [13]. The ecosystem carrying capacity (λ), or the ecosystem function an environment can sustain over time, is adjusted via a normal cumulative density function (CDF, Φ):

$$\Delta\lambda = 1 - 2 \times \Phi\,(\Delta T - \sigma) \tag{5}$$

where σ is the niche breadth of vegetation, or the amount of warming that vegetation can tolerate before regeneration stops. We use the normal CDF to calculate the likelihood that a given change in temperature remains within the tolerance limits specified by an ecosystem's niche breadth. Values close to 1 represent a temperature anomaly within a vegetation's tolerable range and values close to 0 represent a temperature anomaly outside or nearly outside this range. The latter results in a lower carrying capacity because of limits on regenerative potential [13].

In the original HANDY model, natural resources have a fixed carrying capacity (λ). Our $\lambda_{adjusted}$ parameter implements the cumulative density function to limit carrying capacity based on change in temperature:

$$\lambda_{adjusted} = \Delta\lambda \times \lambda \tag{6}$$

which effectively lowers the maximum ecosystem functionality, as well as its ability to regenerate.

Sensitivity Analysis

C^3 is not calibrated to a specific dataset but we instead examine model response across parameter values drawn from literature-informed ranges (see Appendix B, Table A1). We ran a 648-sample sensitivity analysis varying carbon intensity (I_C) and ecological resilience parameters σ, r, and S_{rM} (Table 1), and recorded 1000 simulated years of commoner and elite populations, global mean surface temperature, natural resources, and accumulated wealth. Parameter values were chosen to bracket the range of supported values, and we varied parameters across these ranges to examine model sensitivity to parameter uncertainty.

Table 1. Important C^3 parameters, parameter samples for sensitivity analysis.

Parameter	I_C	σ	r	S_{rM}
Process Represented	Anthropogenic emissions	Critical Thermal Maximum	Decreased photosynthetic Capacity	Carbon Sequestration
Affects	Atmospheric Carbon (Climate)	Adjusted carrying capacity (HANDY)	Atmospheric Carbon (Climate)	Atmospheric Carbon (Climate)
Number of Samples	6	6	3	6
Sample range	{0, 1}	{1, 5}	{0.01, 1, 30}	{0, 0.01}

Carbon intensity samples ranged from 0 to 1 petagrams of carbon per ecodollar per year (Table A1) with a value of 0.4 giving similar cumulative carbon emissions to current society [22]. Niche breadth ranged from tolerating 1 to 5 °C increase from pre-industrial global mean surface temperature (Table A1). Varying this parameter examines the sensitivity of ecosystem function to temperature change, allowing us to see how widening or narrowing niche breadth affects long-term feedbacks between climate change and resources. We used three values of r, which define the functional relationships between temperature and sequestration rate: 30 (rapid initial decline and a limit of zero), 1 (linear), and 0.01 (gradual initial decline followed by acceleration) (Table A1). Finally, the maximum sequestration rate, or the amount of carbon sequestered per ecodollar of natural resources per year, ranged from 0, or no sequestration, to 0.01. Values higher than 0.01 often led to decreasing atmospheric carbon to below equilibrium values, which we deemed not representative of plausible ecological conditions, and therefore truncated the range there (Table A1).

Two regression trees were run on the results of the sensitivity analysis to determine feature importance.

3. Results

3.1. Change in Temperature

The sensitivity analysis yielded clustered temperature change results with clusters largely driven by niche breadth and stratification driven by carbon intensity (Figure 2), as confirmed by a regression tree (Figure 3). Simulations with wider niche breadths tended to yield larger increases in temperature than those with more narrow niche breadths. Similarly, simulations with high values of carbon intensity yielded larger temperature increases than those with low carbon intensity. Functional form and maximum sequestration also drove more granular stratification within these clusters with varying effects. Some simulations

reached equilibria, and some runs peaked and started to decrease between years 2100 and 2250 (Figure 2). A stable temperature equilibrium was achieved in some simulations following societal collapse.

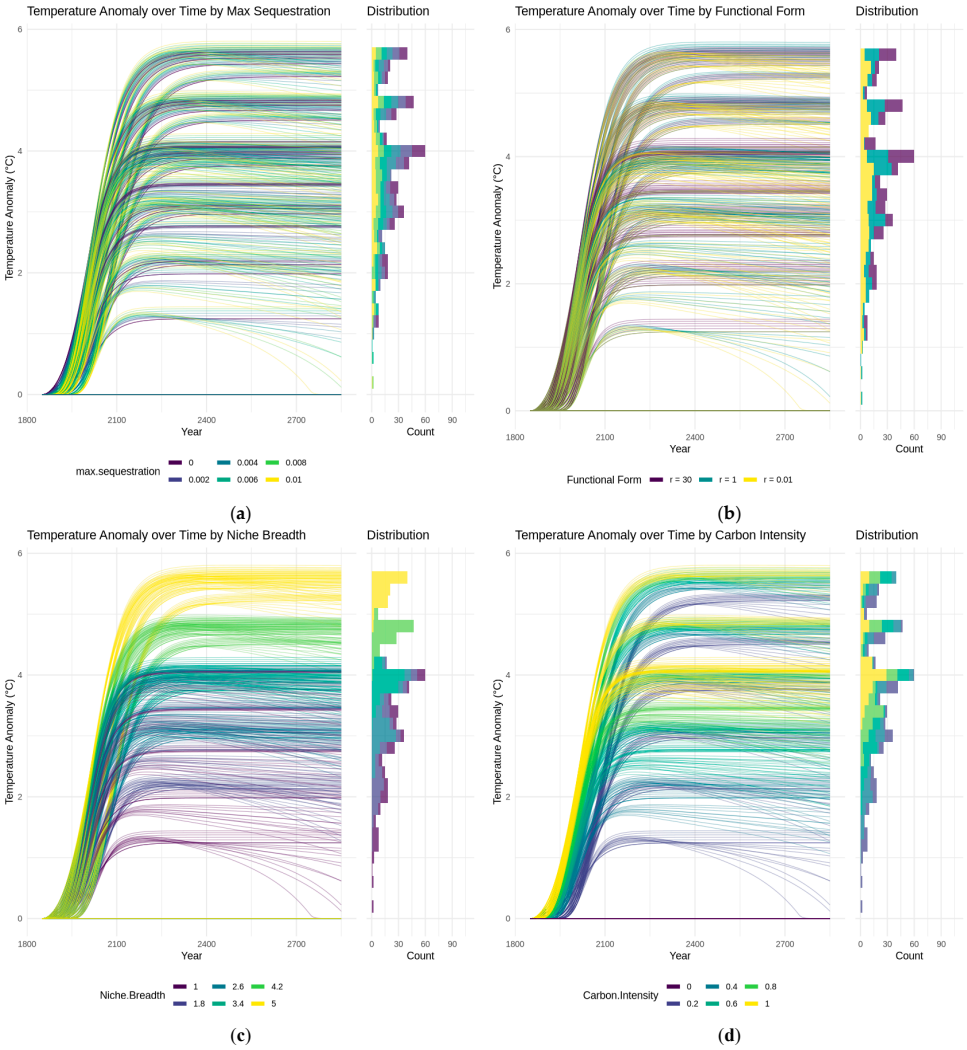

Figure 2. Effect of varied parameters on change in temperature over time. Varied parameters include (**a**) maximum sequestration, (**b**) functional form, (**c**) niche breadth, and (**d**) carbon intensity.

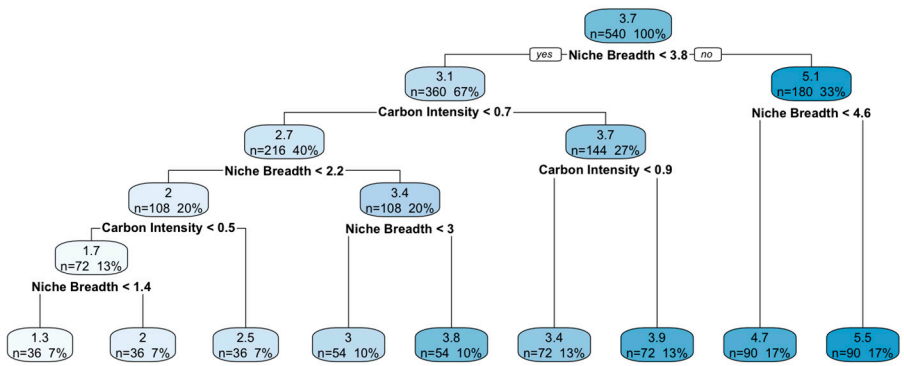

Figure 3. Decision tree identifying parameters associated with the change in global mean surface temperature at the end of 1000 years. Splits represent thresholds in model input variables that best differentiate lower and higher increases in temperature. This figure does not include runs with a carbon intensity of 0.

3.2. Time to Population Collapse

All populations were initially increasing in model simulations (see Appendix C). For each run where GHG emissions were greater than zero ($I_C > 0$), populations peaked around the year 2100 and collapsed before the end of the 1000-year run (Figures A1 and A2). Only populations with no reliance on fossil fuels (i.e., 0 GHG emissions or $I_C = 0$) reached an equilibrium. The inequality factor for all simulations was held constant at 1, and so the proportion of commoners to elites remained at 1:4 for the entire run, and the trajectories of both groups were the same within each run.

There was some clustering in both populations driven by a combination of carbon intensity and niche breadth (Figures A1 and A2). We define collapse as a population with <1 person. Commoner populations that collapsed did so between years 2394 and 2850, with a mean collapse date of 2544 and a median of 2537 (Table A2). The mean collapse time with an I_C of 0.2 was 2649, while a CI of 1 led to a mean collapse time of 2481. The mean collapse time with a niche breadth of 1 was 2430, while a niche breadth of 6 led to a mean collapse time of 2661. As niche breadth widened, both the number of years to collapse and the spread of possible times to collapse increased (Figure 4). Carbon intensity created stratification within this distribution of outcomes, with lower values of carbon intensity delaying collapse (Figure 4). A regression tree examining the time to collapse for commoner populations branched only on niche breadth and carbon intensity (Figure 5).

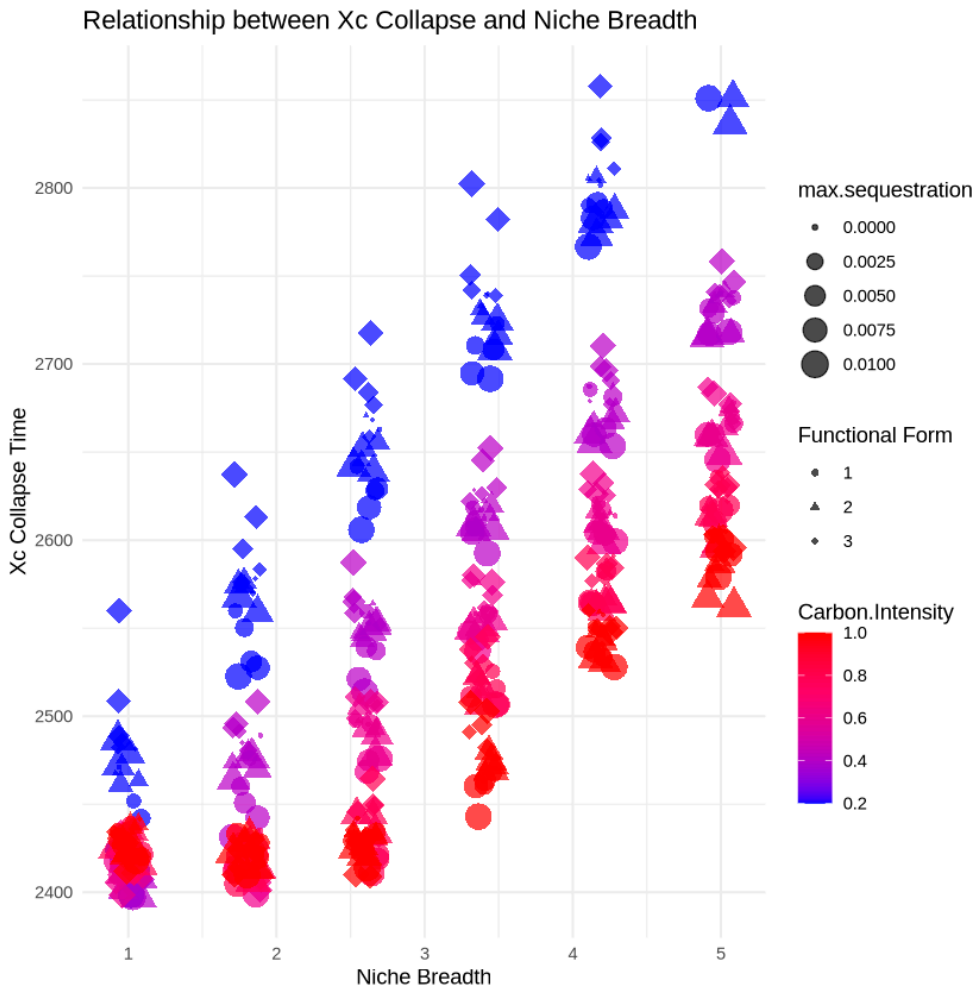

Figure 4. Determinants of year of commoner population collapse with niche breadth represented on the y axis, carbon intensity represented by color, maximum sequestration represented by size, and functional form represented by shape.

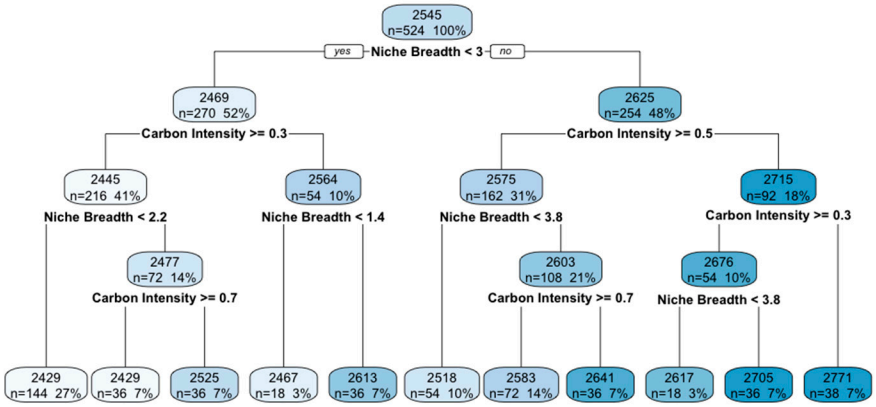

Figure 5. Decision tree identifying parameters associated with the timing of population collapse. Splits represent thresholds in model input variables that best differentiate early versus late collapse outcomes. This figure does not include runs with a carbon intensity of 0.

4. Discussion

4.1. Summary of Findings

We used a coupled model of humans, climate, and ecosystems to examine long-term societal dynamics while varying carbon intensity of the human system and resilience of ecological systems. We found that reinforcing feedbacks between declines in ecosystem function and climate change amplified overshoot of human carrying capacity. Our simulations illustrate the potential effects of continued GHG emissions on societal outcomes. Net emissions greater than 0 led to societal collapse in all of our simulations, with higher carbon intensities leading to earlier collapse. The combined effects of GHG emissions and ecological stress in our model simulations reinforces the need for timely reductions in anthropogenic emissions with a goal of net-zero emissions.

Reducing GHG emissions is the most immediate and actionable step society can take to delay collapse. Our results also illustrate that societal outcomes also depend on ecological resilience—especially niche breadth which, in our C^3 model, reflects how much climatic change ecosystems can tolerate before their function declines. Increases in global temperature are a consequence of any amount of GHG emissions, and so the ability of ecological systems to function in the face of climate change is a critical factor in societal resilience or collapse. This points to the need for a concomitant focus on fostering ecological resilience to climate change in addition to achieving net-zero GHG emissions.

4.2. Paradox of Resilience

Counterintuitively, a narrow niche breadth in our model simulations led to lower overall temperature increases than did wide niche breadth. This is because a narrow niche breadth was associated with faster resource depletion and societal collapse, which in turn meant less overall anthropogenic GHG emissions. In contrast, when niche breadth was wide, ecosystems could tolerate relatively more climate change, which supported larger human populations and economic activity, and ultimately led to more GHG emissions and increased climate change. Greater ecosystem resilience allows society to emit more GHGs and drive more climate change before societal collapse. This apparent paradox, that greater ecosystem resilience allows humans to engage in unsustainable behaviors for longer before ecological systems collapse, could provide time and opportunity to achieve sustainability, but could also be mistakenly interpreted as society being resilient and sustainable. This is reminiscent of the observation that those societies most responsible for emissions often avoid their most immediate effects [23] and represents a potential "system trap" of high ecosystem resilience.

Although high levels of ecological resilience and lowered dependence on fossil fuels may postpone societal collapse, any net emissions of GHGs inevitably lead to societal collapse. The implication is that the use of non-renewable fossil fuels can make renewable resources less renewable: In our C^3 model simulations, GHG emissions reduced the resilience of ecological systems, reducing the regeneration of renewable resources.

4.3. Limitations and Future Directions

Our C^3 model is a greatly simplified Earth system model that does not account for many important processes, for example, socio-behavioral feedbacks to GHG emissions, technological development that reduces carbon intensity of economic activities, and regional variation in ecological impacts that could affect global ecological resilience. Our model is nonspatial and so does not account for regional variation in climate change nor variation in ecosystem function. Other unrepresented effects on ecological function could arise with warming as well, including increased incidence of disease [24], natural disasters [25], and heat waves [26], which in turn could directly affect population sizes. Finally, our model does not explicitly include the socio-behavioral effects of climate change, societal derailment, and political instability sparked by resource insecurity [17], nor perceived risk and policy interventions that continued climate change may bring about [27,28]. Our C^3 model presents a simplified and abstract representation of ecosystem resilience that allows us to examine feedbacks between ecosystems, humans, and climate using a low-dimensional model to better understand interactions between system components. Technological advancements, dynamic socio-behavioral responses and changing ecological responses that reduce GHG emissions over time are not included in the model, though a dynamic carbon intensity parameter would only delay collapse in the absence of achieving 0 net emissions. For projections or predictions of likely societal trajectories, more complex and complete representations of ecological, social, or economic systems would be needed.

Our model is a mean field approximation that does not include spatial heterogeneity, which can lead to complex feedbacks between emissions and the impacts of climate change mediated by the human perception of risk, and more complex ecosystem responses that could impact system resilience. Future enhancements to our model could include adding spatial heterogeneity, human behavioral components, international policy or climate interventions [28], or explicit economic models [29]. Inequality or consumption rates can also be varied alongside our case of an equitable society, as in Motesharrei et al., to examine how socioeconomic inequality affects system behavior [1]. These increases in model complexity could allow the model to better explore the effects of economic, social, geographical, and political heterogeneity on ecosystem–climate feedbacks.

5. Conclusions

Historically, societal collapse could often be attributed to overutilization of localized resources. Today, societal impacts on global climate mean that our models must account for the compounding effects of reinforcing feedbacks between ecosystem function and climate change. Integrating climate change into socio-ecological models is crucial for capturing these feedbacks. We expanded upon an existing societal collapse model to include the impacts of climate change. In our simulations, reinforcing feedbacks between climate change and ecological systems amplified the effects of societal overshoot. Higher carbon intensity of economic activities led to faster resource depletion because of declining ecosystem function driven by climate change, accelerating societal collapse. While reducing fossil fuel use to net-zero emissions is a necessary step to achieving a sustainable society, our simulation outcomes were also dependent on ecosystem resilience to climate change.

Conservation and management of ecosystems can also bolster resilience of ecosystem services and contribute to long-term sustainability of the coupled human and Earth system.

Author Contributions: Conceptualization, B.B.; methodology, G.S. and B.B.; software, G.S. and G.B.; validation, G.S.; formal analysis, G.S.; investigation, G.S.; resources, G.S., G.B. and B.B.; data curation, G.S.; writing—original draft preparation, G.S. and G.B.; writing—review and editing, G.S. and B.B.; visualization, G.S.; supervision, B.B. All authors have read and agreed to the published version of the manuscript.

Funding: B.B. was supported by the USDA National Institute of Food and Agriculture Hatch, Project Number 1025208 and National Science Foundation Award Number 2436120. G.S. was supported by grant number 80NSSC20M0122 from the National Aeronautics and Space Administration.

Data Availability Statement: Model available in a publicly accessible repository at: https://exchange.iseesystems.com/models/player/greta-savitsky/population-climate-model (accessed on 10 August 2025).

Acknowledgments: We gratefully acknowledge the helpful feedback from two reviewers and the editor. We used ChatGPT-4o to provide feedback on manuscript drafts, and to assist with spelling and grammar, and Julius AI for formatting figures. The authors have reviewed and edited the output and take full responsibility for the content of this publication.

Conflicts of Interest: The authors declare no conflicts of interest.

Abbreviations

The following abbreviations are used in this manuscript:

GHG	Greenhouse gas
HANDY	Human and Nature Dynamics

Appendix A

Appendix A.1. Predator-Prey Model

This simple predator prey model describes the relationship between the two species, predator and prey, using the following system of equations:

$$x = (ay)x - bx \tag{A1}$$

$$y = cy - (dx)y \tag{A2}$$

where x is the predator species, y is the prey species, a is the birth rate of the predator, b is the death rate of the predator, c is the birthrate of the prey, and d is the rate of predation, or the rate which the prey is hunted by the predator. The predator-prey model is famous for its oscillatory behavior, with each species showing periodic, out-of-phase variations around their equilibrium values:

$$xe = c/d \tag{A3}$$

$$ye = b/a \tag{A4}$$

Appendix A.2. HANDY Model

Populations grow through birth rate β and decrease through death rate α. α is dependent on the amount of available natural resources, increasing to αm to simulate famine.

$$X_C = \beta_C X_C - \alpha_C X_C \tag{A5}$$

$$X_E = \beta_E X_E - \alpha_E X_E \tag{A6}$$

$$y = \gamma y(\lambda - y) - \delta X_C\, y \tag{A7}$$

$$w = \delta X_C y - C_C - C_E) \tag{A8}$$

Natural resources are increased through regeneration $\gamma y\ (\lambda - y)$ proportionally to regeneration term γ and saturated at Nature's carrying capacity λ. Nature is decreased through $\delta X_C y$, proportional to the commoner population that is using the resources a depletion factor δ. HANDY considers the concept of wealth accumulation, or accumulation of resources. The accumulated wealth stock increases by natural resource depletion δX_C and is decreased by commoner and elite consumption rates (C_C and C_E), defined by salary and class. The consumption of commoners is sX_C, a subsistence salary per capita. Elite consumption is κ times larger.

$$C_C = (1, w/wth)sX_C \tag{A9}$$

$$C_E = (1, w/wth)\kappa sX_E \tag{A10}$$

where s is the subsistence salary per capita and κ is the inequity factor between commoners and elites. However, when wealth is depleted beyond the threshold wealth, determined by the minimum required consumption per capita ρ,

$$wth = \rho xC + \kappa \rho xE \tag{A11}$$

society experiences famine, meaning consumption decreases and death rates increase to α_M. This can be caused by several reasons, such as an increase in susceptibility for disease, a lack of food, or violence within the society [1]. Death rates for commoners and elites are represented through the following functions:

$$\alpha_C = \alpha_m + \max\,(0, 1 - C_C\, sx_C)(\alpha_M - \alpha_m) \tag{A12}$$

$$\alpha_E = \alpha_m + \max\,(0, 1 - CE\, sx_E)(\alpha_M - \alpha_m) \tag{A13}$$

Appendix A.3. Climate Model

The gray atmosphere component of the climate model takes in global albedo, incoming solar radiation (solar constant, S), and the opacity of the atmosphere, and outputs the total solar flux that reaches the Earth's surface (Fd) in W m^{-2}. Fd increases inversely to albedo as more light is reflected back to space and increases proportionally to atmospheric opacity (τ). Fd increases inversely to albedo as more light is reflected back to space, and increases proportionally to atmospheric opacity (τ):

$$Fd = (((1 - \rho) \times S)/4) \times (1 + ¾ \times \tau) \tag{A14}$$

As atmospheric opacity increases, more radiation is trapped inside the atmosphere, leading to a higher total solar flux reaching the Earth's surface. This is known as the greenhouse effect [18]. The opacity of the atmosphere (τ) is determined by adding the opacity of three atmospheric gases: carbon dioxide (CO_2), water vapor (H_2O), and methane (CH_4):

$$\tau = \tau(CO_2) + \tau(H_2O) + \tau(CH_4) \tag{A15}$$

A constant level of methane, and therefore a constant opacity at 0.0231, is assumed for the model. Water vapor opacity increases with temperature as water vapor pressure

(PH_2O) increases. Water vapor pressure is calculated at each time step as a function of average global surface temperature (T) and relative humidity (H):

$$P(H_2O) = H \times (P_0 e^{-(L/RT)}) \quad (A16)$$

where R is the molar gas constant (8.314 J mol^{-1} K^{-1}), L is the latent heat per mole of water (43,655 J mol^{-1}), P_0 is a constant for the water vapor saturation curve (1.4×10^{11} Pa), T is temperature and H is relative humidity. Subsequently, the opacity of atmospheric water vapor is derived from its pressure:

$$\tau(H_2O) = 0.0126 \times P(H_2O)^{0.503} \quad (A17)$$

The opacity of CO_2 is calculated as a function of total atmospheric CO_2 (C_A) in ppm:

$$\tau(CO_2) = 1.73 \times (pCO_{2(A)})^{0.263} \quad (A18)$$

where $pCO_{2(A)}$ is the atmosphere mixing ratio of CO_2, and is defined as a function of Ca and the total number of molecules in the atmosphere (ka)

$$pCO_{2(A)} = C_A / ka \quad (A19)$$

where ka = 1.772×10^{20}, and is assumed to be independent of C_A.

Appendix B

Supplemental Results

Table A1. Parameter samples for sensitivity analysis.

Parameter	I_C	σ	r	S_{rM}
Sample range	{0, 1}	{1, 5}	{0.01, 1, 30}	{0, 0.01}
Justification	After running shortened simulations from 1850 to 2022, we found that a value of 0.4–0.5 led to similar anthropogenic emissions to observed data since the industrial revolution. Therefore, we made 0.5 the mean value of CI. We chose 0 as a lower bound to show the impact of net-zero GHG emissions, and 1 as the upper bound to show extreme GHG emission scenarios and keep the mean sample at 0.5.	We chose this range to represent realistic warming scenarios over the next 1000 years. We also use this range to test a variety of possible "tipping point" temperatures (at which reinforcing ecological feedbacks begin) proposed by Armstrong McKay et al., (2022).	The range of r designates the functional form of the relationship between temperature and ecosystem function. We use photosynthetic capacity, as we are specifically interested in how climate change might limit carbon sequestration. The three values represent extreme possibilities of this functional relationship, including steep exponential decay with increasing temperatures, linear decay, and gradual logistic decay.	The maximum sequestration rate, or the rate at which natural resources can sequester carbon, is a representation of the maximum functional capacity of ecosystem services in terms of carbon sequestration. We bookended the range of tested values with 0, or no carbon sequestration, and 0.01, which often yielded unrealistically low atmospheric carbon concentrations
Source	[22]	[12,30]	None	[30]

Appendix C

Supplemental Results

Table A2. Mean time to collapse across values of carbon intensity (CI) and niche breadth (σ).

	Carbon Intensity		
Niche Breadth	0.2	0.6	1
1	2466.6	2421.1	2427.7
2.6	2654.9	2497.7	2423.9
5	2845.3	2667.2	2591.6

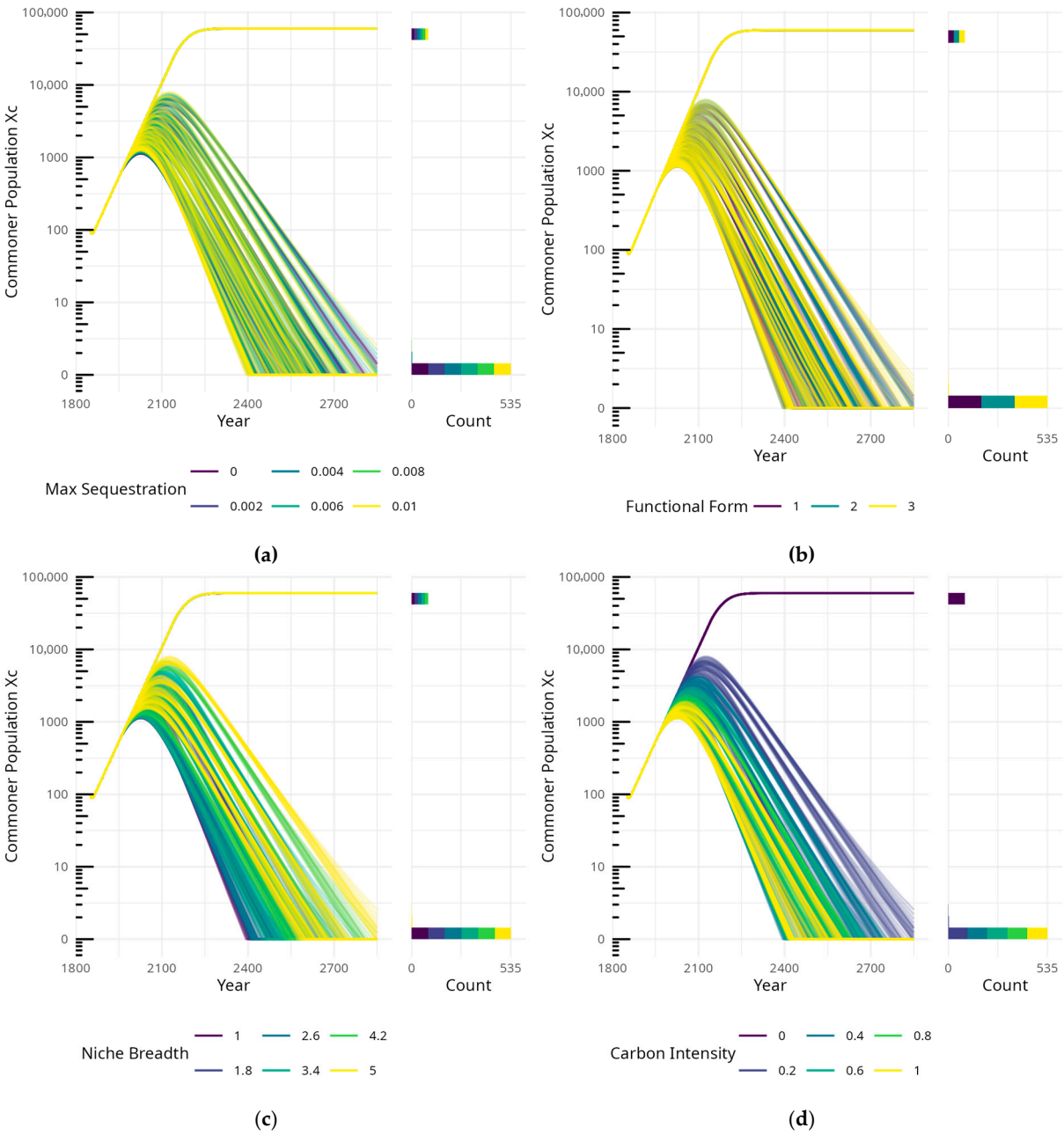

Figure A1. Effect of varied parameters (**a**) maximum sequestration, (**b**) functional form, (**c**) niche breadth, and (**d**) carbon intensity on commoner population over time.

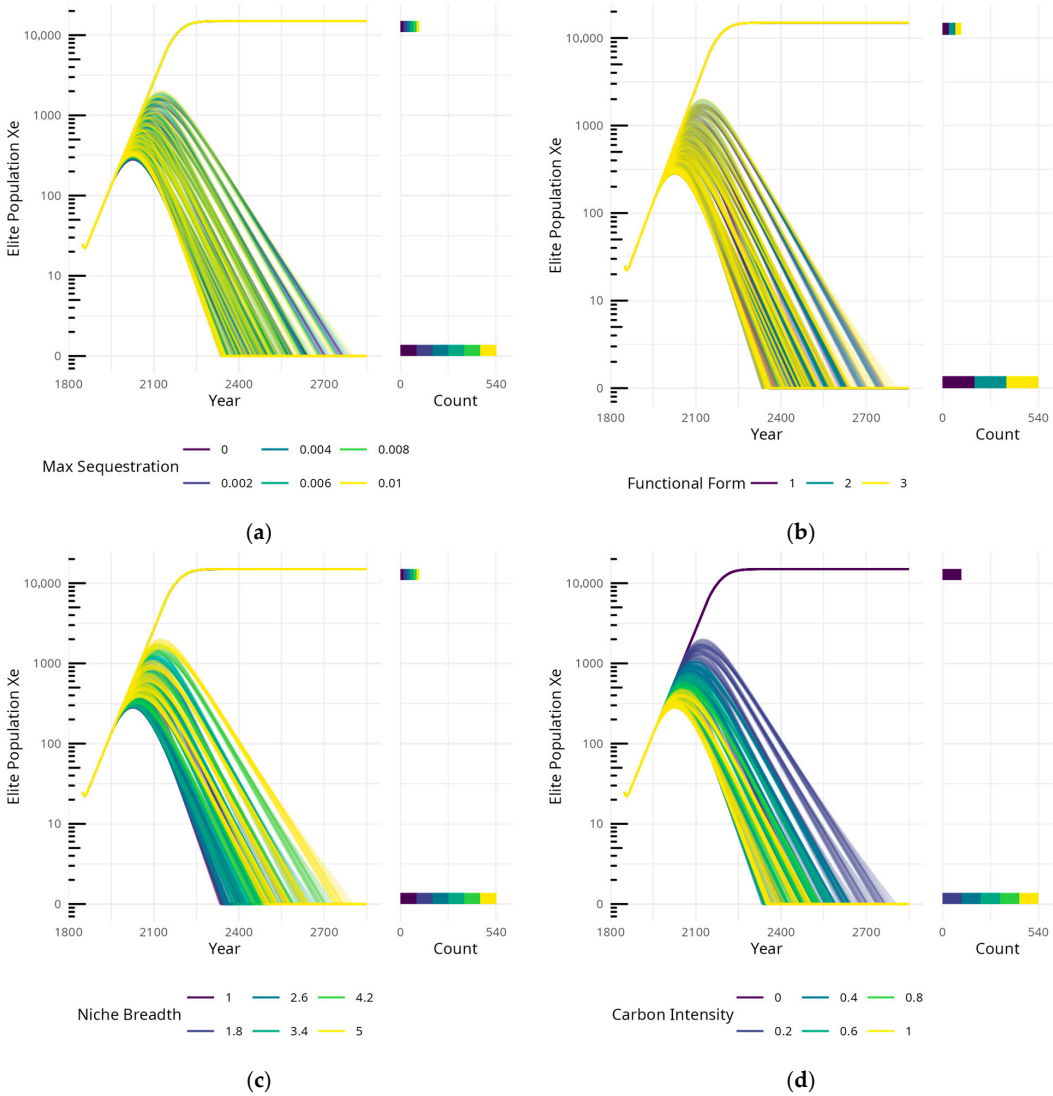

Figure A2. Effect of varied parameters (**a**) maximum sequestration, (**b**) functional form, (**c**) niche breadth, and (**d**) carbon intensity on elite population over time.

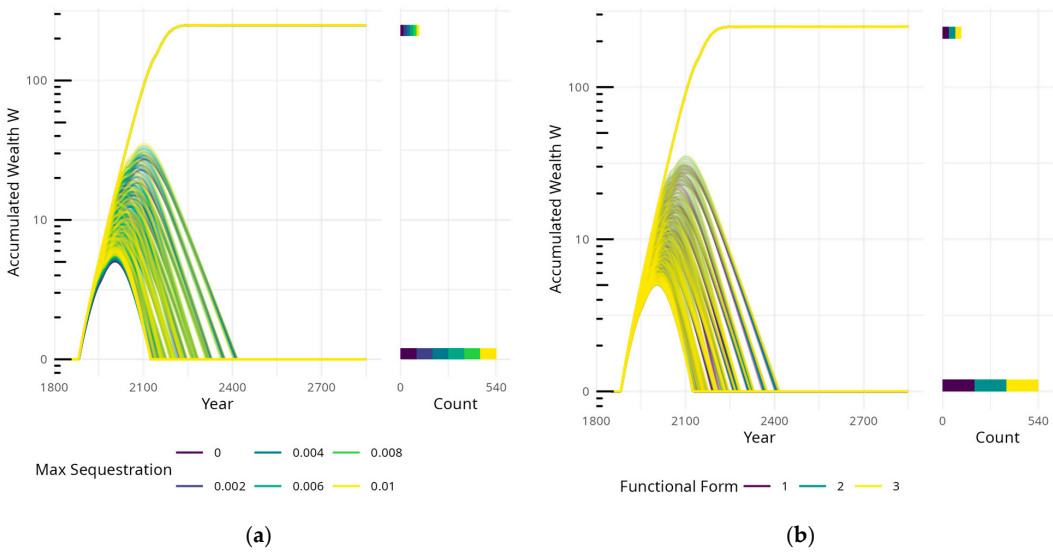

Figure A3. *Cont.*

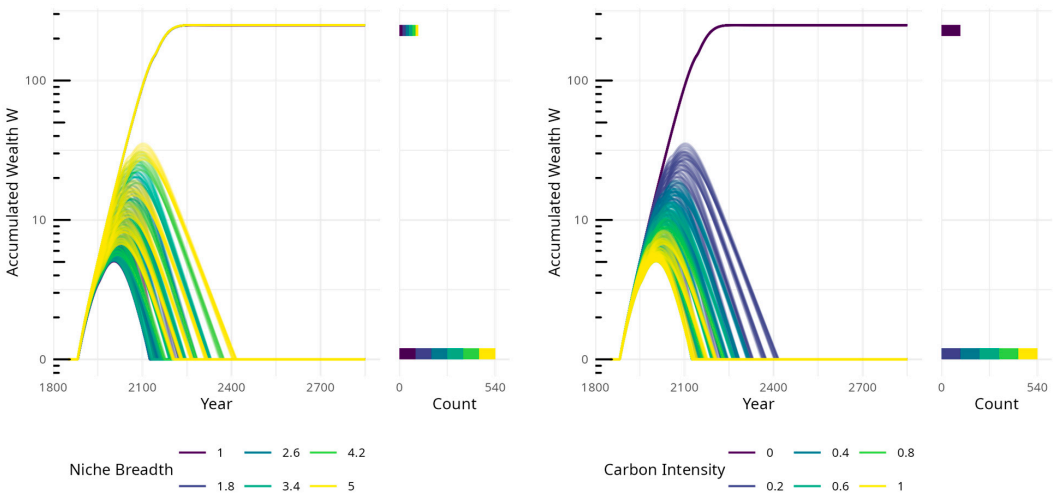

(**c**) (**d**)

Figure A3. Effect of varied parameters (**a**) maximum sequestration, (**b**) functional form, (**c**) niche breadth, and (**d**) carbon intensity on accumulated wealth over time.

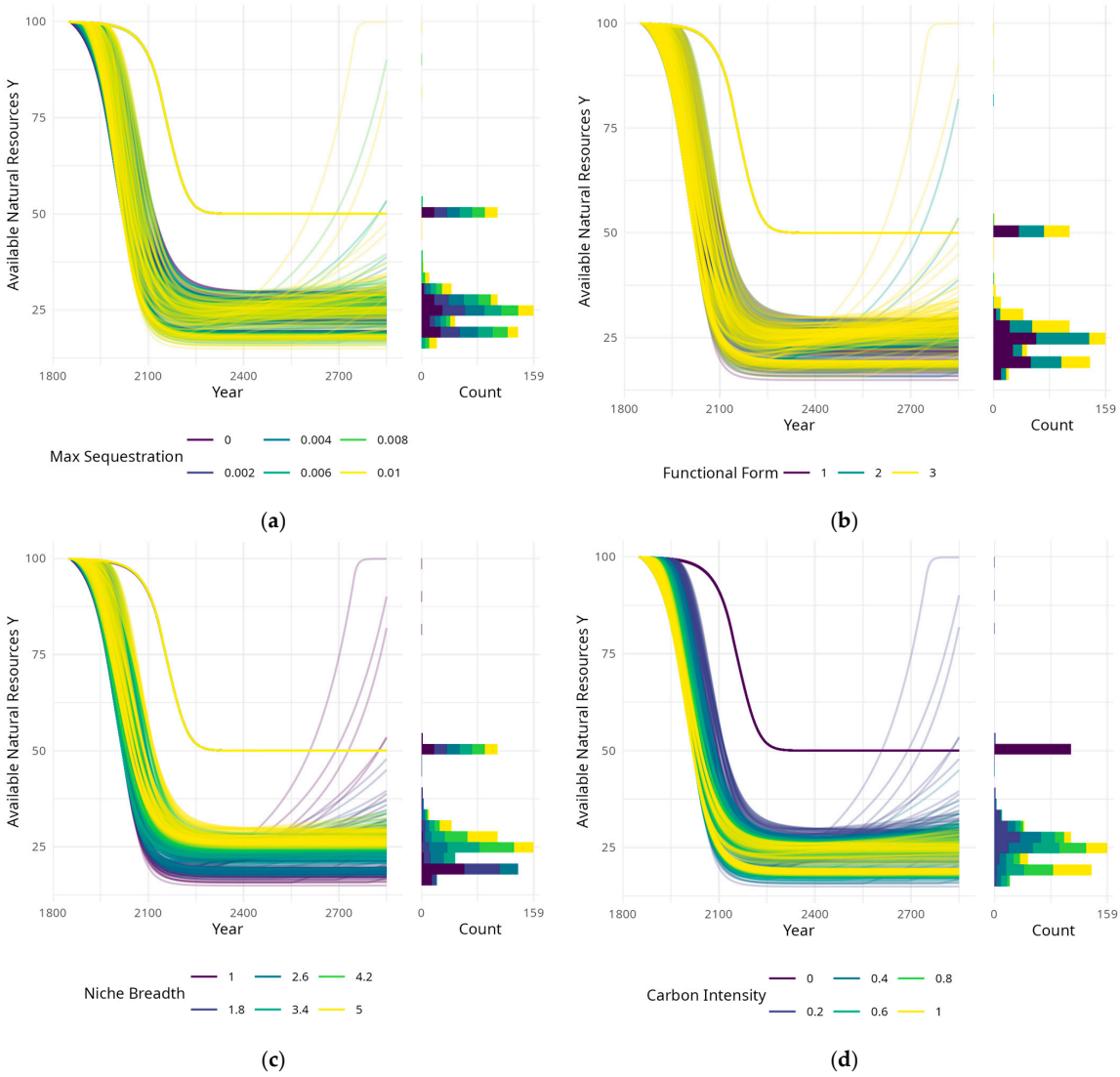

(**a**) (**b**)

(**c**) (**d**)

Figure A4. Effect of varied parameters (**a**) maximum sequestration, (**b**) functional form, (**c**) niche breadth, and (**d**) carbon intensity on natural resources over time.

References

1. Motesharrei, S.; Rivas, J.; Kalnay, E. Human and nature dynamics (HANDY): Modeling inequality and use of resources in the collapse or sustainability of societies. *Ecol. Econ.* **2014**, *101*, 90–102. [CrossRef]
2. Meadows, D. *Thinking in Systems*; Chelsea Green Publishing: White River Junction, VT, USA, 2008.
3. Daily, G.C.; Ehrlich, P.R. *Population, Sustainability, and Earth's Carrying Capacity*; Springer: New York, NY, USA, 1992.
4. Diamond, J.M. *Collapse: How Societies Choose to Fail or Succeed*; Viking: New York, NY, USA, 2005.
5. Tainter, J.A. *The Collapse of Complex Societies*; Cambridge University Press: Cambridge, UK, 1988.
6. Malthus, T. *An Essay on the Principle of Population*; Oxford University Press: London, UK, 1798.
7. Hardin, G. The Tragedy of the Commons. *Sci. New Ser.* **1968**, *162*, 1243–1248. [CrossRef] [PubMed]
8. Catton, W.R. *Overshoot: The Ecological Basis of Revolutionary Change*; Board of Trustees of the University of Illinois Press: Champaign, UK, 1980.
9. McKibben, B. *Eaarth: Making a Life on a Tough New Planet*, 1st ed.; Martin's Griffin: New York, NY, USA, 2011.
10. Kolbert, E. *The Sixth Extinction: An Unnatural History*; Henry Holt and Company: New York, NY, USA, 2014.
11. Steel, D.; DesRoches, C.T.; Mintz-Woo, K. Climate change and the threat to civilization. *Proc. Natl. Acad. Sci. USA* **2022**, *119*, e2210525119. [CrossRef] [PubMed]
12. Armstrong McKay, D.I.A.; Staal, A.; Abrams, J.F.; Winkelmann, R.; Sakschewski, B.; Loriani, S.; Fetzer, I.; Cornell, S.E.; Rockström, J.; Lenton, T.M. Exceeding 1.5 °C global warming could trigger multiple climate tipping points. *Science* **2022**, *377*, eabn7950. [CrossRef] [PubMed]
13. Parker, L.E.; McElrone, A.J.; Ostoja, S.M.; Forrestel, E.J. Extreme heat effects on perennial crops and strategies for sustaining future production. *Plant Sci.* **2020**, *295*, 110397. [CrossRef] [PubMed]
14. White, A.; Cannell, M.G.R.; Friend, A.D. Climate change impacts on ecosystems and the terrestrial carbon sink: A new assessment. *Glob. Environ. Chang.* **1999**, *9*, S21–S30. [CrossRef]
15. Seidl, R.; Thom, D.; Kautz, M.; Martin-Benito, D.; Peltoniemi, M.; Vacchiano, G.; Wild, J.; Ascoli, D.; Petr, M.; Honkaniemi, J.; et al. Forest disturbances under climate change. *Nat. Clim. Chang.* **2017**, *7*, 395–402. [CrossRef] [PubMed]
16. Fowler, C.; Westengen, O.T. Climate change, food and biodiversity. In *Biodiversity and Climate Change: Transforming the Biosphere*; Lovejoy, T.E., Hannah, L., Eds.; Yale University Press: New Haven, CT, USA, 2019; pp. 347–355.
17. Richards, C.E.; Lupton, R.C.; Allwood, J.M. Re-framing the threat of global warming: An empirical causal loop diagram of climate change, food insecurity and societal collapse. *Clim. Change* **2021**, *164*, 49. [CrossRef]
18. Lenton, T.M. Land and ocean carbon cycle feedback effects on global warming in a simple Earth system model. *Tellus B Chem. Phys. Meteorol.* **2000**, *52*, 1159. [CrossRef]
19. Lotka, A.J. *Elements of Physical Biology*; Williams & Wilkins: Philadelphia, PA, USA, 1925.
20. Volterra, V. *Variazioni e Fluttuazioni del Numero D'individui in Specie Animali Conviventi*; Società anonima tipografica Leonardo da Vinci: Città di Castello, Italy, 1926.
21. Zahra, N.; Hafeez, M.B.; Ghaffar, A.; Kausar, A.; Zeidi, M.A.; Siddique, K.H.M.; Farooq, M. Plant photosynthesis under heat stress: Effects and management. *Environ. Exp. Bot.* **2023**, *206*, 105178. [CrossRef]
22. Thoning, K.W.; Crotwell, A.M.; Mund, J.W. *Atmospheric Carbon Dioxide Dry Air Mole Fractions from Continuous Measurements at Mauna Loa, Hawaii, Barrow, Alaska, American Samoa and South Pole, 1973–Present*; Version 2025-04-26; National Oceanic and Atmospheric Administration (NOAA), Global Monitoring Laboratory (GML): Boulder, CO, USA, 2025. [CrossRef]
23. Schöngart, S.; Nicholls, Z.; Hoffmann, R.; Pelz, S.; Schleussner, C.-F. High-income groups disproportionately contribute to climate extremes worldwide. *Nat. Clim. Change* **2025**, *15*, 627–633. [CrossRef]
24. Lafferty, K.D. The ecology of climate change and infectious diseases. *Ecology* **2009**, *90*, 888–900. [CrossRef] [PubMed]
25. Van Aalst, M.K. The impacts of climate change on the risk of natural disasters. *Disasters* **2006**, *30*, 5–18. [CrossRef] [PubMed]
26. Mitchell, D.; Heaviside, C.; Vardoulakis, S.; Huntingford, C.; Masato, G.; PGuillod, B.; Frumhoff, P.; Bowery, A.; Wallom, D.; Allen, M. Attributing human mortality during extreme heat waves to anthropogenic climate change. *Environ. Res. Lett.* **2016**, *11*, 074006. [CrossRef]
27. Beckage, B.; Gross, L.J.; Lacasse, K.; Carr, E.; Metcalf, S.S.; Winter, J.M.; Howe, P.D.; Fefferman, N.; Franck, T.; Zia, A.; et al. Linking models of human behaviour and climate alters projected climate change. *Nat. Clim. Chang.* **2018**, *8*, 79–84. [CrossRef]
28. Beckage, B.; Lacasse, K.; Raimi, K.T.; Visioni, D. Models and scenarios for solar radiation modification need to include human perceptions of risk. *Environ. Res. Clim.* **2025**, *4*, 023003. [CrossRef]

29. Nordhaus, W.D. *The 'DICE' Model: Background and Structure of a Dynamic Integrated Climate-Economy Model of the Economics of Global Warming*; Cowles Foundation Discussion Papers 1009, Cowles Foundation for Research in Economics; Yale University: New Haven, CT, USA, 1992.
30. Foster, G.; Ahn, J.; Hall, B.; Quaas, J. Technical Summary of the Working Group I Contribution to the IPCC Sixth Assessment Report—Data for Figure TS.9 v20220922. NERC EDS Centre for Environmental Data Analysis, 27 July 2023. Available online: https://doi.org/10.5285/f99ec964a6f345beadb000e295ac2e5b (accessed on 9 May 2025).

Disclaimer/Publisher's Note: The statements, opinions and data contained in all publications are solely those of the individual author(s) and contributor(s) and not of MDPI and/or the editor(s). MDPI and/or the editor(s) disclaim responsibility for any injury to people or property resulting from any ideas, methods, instructions or products referred to in the content.